Journal of Metals, Materials and Minerals, 34(2), 1984, 2024

Natural wound dressing films prepared from acetylated starch/κ-carrageenan blend incorporated with mandelic acid

Wimolsiri SRIPHOCHAI[1], and Jutarat PRACHAYAWARAKORN[1,2*]

[1] *Department of Chemistry, School of Science, King Mongkut's Institute of Technology Ladkrabang (KMITL), Bangkok 10520, Thailand*
[2] *Advanced Materials Research Unit, School of Science, King Mongkut's Institute of Technology Ladkrabang (KMITL), Bangkok 10520, Thailand*

***Corresponding author e-mail**: jutarat.si@kmitl.ac.th

Received date:
5 March 2024
Revised date
10 April 2024
Accepted date:
25 April 2024

Keywords:
Acetylated starch;
κ-Carrageenan;
Mandelic acid;
Modification;
Wound dressing

Abstract

Due to several limitations of acetylated starch film for wound dressing applications such as low mechanical properties and no antibacterial activity, acetylated starch film was, therefore, modified by different contents of κ-carrageenan and mandelic acid. Infrared spectra confirmed the presence of κ-carrageenan and mandelic acid in the modified acetylated starch films. In addition, the decreased crystallinity of the carrageenan modified acetylated starch films led to more smooth film, as observed by scanning electron images. Besides, the addition of various amounts of κ-carrageenan in the modified acetylated starch films caused the improvement of mechanical properties, moisture uptake, water vapor transmission rate (WVTR), and degree of swelling. Moreover, κ-carrageenan modified acetylated starch film loaded with 20 wt% of mandelic acid exhibited antibacterial property against both S.aureus and E.coli bacteria. Additionally, degree of crystallinity, mechanical properties, moisture uptake, WVTR, degree of swelling, antibacterial activity, and cytotoxicity of κ-carrageenan modified acetylated starch films added by different amounts of mandelic acid were also studied.

1. Introduction

The ideal wound dressing for wound healing should serve several purposes. Firstly, it should promote a moist healing environment by allowing appropriate steam to pass through helping to absorb excess fluid and inflammation from the wound. The wound dressing should also possess antioxidant and antimicrobial properties to prevent infection and support the healing process. It should also be bio-degradable and biocompatible, ensuring compatibility with the body's tissues. Lastly, the wound dressing should be easily detachable from the wound surface [1]. Natural wound dressing films can be made from various biopolymers such as chitosan, gelatin, starch, etc [2].

Starch is a widely studied raw material that has gained significant attention for several reasons. It is valued for its low production cost, abundant availability, biodegradability, and various desirable properties, such as being odorless, colorless, and non-toxic [3,4]. The natural form of starch has limited utility because of its properties. However, through modification, starch can be enhanced and made more versatile. Among the various modifications such as oxidation, esterification, etherification, etc, acetylation has received significant attention in starch research [5].

The use of acetylated starch (AS) in food applications has gained interest due to its thickening properties. For food applications, acetyl groups are introduced at a relatively low level. The maximum allowable degree of substitution (DS) is 0.2, for acetylated starches as assigned by US Food and Drug Administration (FDA) in 1980 [6]. AS can be prepared via esterification, i.e. acetylation by acetic acid, acetic anhydride, ketone, or vinyl acetate. Acetylation replaces hydroxyl groups of starch with acetyl groups, which reduces bond strength between the starch chains [7]. This caused the increase of swelling and solubility properties, the decrease of retrogradation, and the improvement of clarity (DS = 0.03-0.08) [8]. It was reported that mechanical properties of AS decreased when DS was increased (0.03 to 0.05) [9]. In order to improve its functional properties of AS film, such as poor mechanical properties and degree of swelling, the addition of another polymer with AS is an interesting approach.

AS has been mentioned to be blended by several types of polymers, for example polyvinyl alcohol (PVA) and chitosan. It was found that when PVA content was increased, elastic modulus, tensile strength, elongation, and degree of swelling of AS/PVA films increased and oil permeability reduced [10]. Moreover, water vapor permeability of AS/chitosan films decreased with increasing chitosan content [11].

Furthermore, carrageenan is one of the biopolymers that can blend with AS. Carrageenan is a linear polysaccharide with sulfated groups in the molecule, commonly found in intercellular matrix and cell walls of various red seaweed species. The main structure of carrageenan consists of alternating disaccharide repeating units, with ß-D-galactose at position 3 and α-D-galactose at position 4. Carrageenan can be categorized into three types based on 3,6-anhydrogalactose, the position and number of sulfated groups: kappa (κ), iota (ι), and lambda (λ) carrageenan [12]. Carrageenan has been widely applied in several industries, such as thickeners, stabilizers, emulsifiers, gelling agents, and non-toxic ingredients in food, toothpaste, shampoo, and cosmetics, due to its high hydrophilicity, mechanical

strength, and biocompatibility. Additionally, the gelling property of carrageenan further enhanced the film stability [13-15]. It was mentioned that the addition of κ- carrageenan led to the increase of tensile strength and water solubility of thermoplastic starch because of hydrogen bond formation between starch and κ-carrageenan [16]. Furthermore, tensile strength, degree of swelling, water vapor permeability and water solubility of agar/ κ-carrageenan blend tended to increase with the increasing content of κ-carrageenan [17]. Furthermore, tensile strength, elastic modulus and degree of swelling of κ-carrageenan /cassava starch/PVA films increased with increasing κ-carrageenan content [18]. Therefore, blending κ-carrageenan could increase the good mechanical properties and degree of swelling of AS film.

In addition, antimicrobial activity is one of the important characteristics for wound dressing. Therefore, several studies have been investigated on improving the antibacterial activity of wound dressing films to expand the use of wound dressing application. Phenolic compounds have been recognized for their effective antibacterial and antioxidant properties, making them interesting candidate for medical and pharmaceutical applications [19]. One way to enhance the antibacterial activity of wound dressing films is to use phenolic acid, such as benzoic acid or mandelic acid (MA). MA is an optically active α-hydroxy acid with the chemical formula $C_8H_8O_3$. It is classified within a group of compounds that contain an aromatic ring in their structure. With a pKa value of 3.4, MA exhibits acidic properties. Its natural source can be obtained from almonds, apricots, and cherries. MA finds applications in various medical and peri-medical fields, particularly dermatology, pharmacy, and cosmetology [20]. It was mentioned that the incorporation of MA in soy protein-based films caused the improvement of antibacterial activity, against *E.coli* [21,22]. In addition, MA also exhibited effective antibacterial property against *S.aureus* bacteria [23].

To the best of our knowledge, there has been no report for natural films prepared from AS/κ- carrageenan blend incorporated by MA for wound dressing application. Fourier-transform infrared (FTIR) spectroscopy, X-ray diffraction (XRD) and scanning electron microscopy (SEM), were used to characterize all AS modified films. In addition, mechanical property, moisture uptake, water vapor transmission rate (WVTR), degree of swelling, antibacterial activity, and cytotoxicity were also determined.

2. Experimental

2.1 Materials

Native cassava starch was purchased from E.T.C. Eaibtongchan Co., Ltd (Nonthaburi, Thailand). Vinyl acetate monomer (VA) (AR grade ≥99.0%) was received from Tokyo Chemical Industry Co., Ltd (Tokyo Japan). κ-carrageenan (CAR) (particle size of less than 250 μm, Commercial grade) and MA (Cosmetic grade) were obtained from Krungthepchemi CO., Ltd (Bangkok, Thailand) and Canjao Lomgevity CO., Ltd (Bangkok, Thailand), respectively. Glycerol (Food grade ≥99.7%) was procured from Chemipan Co., Ltd (Bangkok, Thailand). Sodium hydroxide and Hydrochloric acid were AR grade.

2.2 Preparation of AS

The acetylation (esterification) for cassava starch was performed following to the technique outlined by Raina *et al.* [24]. Briefly, cassava starch (162 g) was suspended in distilled water (220 mL) and stirred until the starch suspension was formed at room temperature. pH of the solution was adjusted to 8.0 using NaOH (3% w/v), and VA was, then, added to the solution while pH was maintained between 8.0 and 8.4 by adding NaOH at room temperature. The reaction was terminated by adjusting pH to 4.5 using HCl (0.5 M). After that, the filtered product was then washed five times with distilled water before being dried at 60°C for 8 h. Finally, the product was milled, sieved (70 μm), and stored for further use.

DS of the prepared AS was carried out according to Kalita *et al.* [25]. The process involved dispersing 5 g of AS starch in 50 mL of distilled water, adding phenolphthalein indicator and titrating with NaOH (0.1 M) until a permanent pink color was achieved. Then, 25 mL of NaOH (0.45 M) was incorporated to the mixture and shaken vigorously for 30 min. The excess alkali was neutralized by back titration with HCl (0.2 M) until the pink color disappeared. DS of the prepared AS was 0.08 ± 0.01, classified as low DS.

2.3 Preparation of AS and modified AS films

AS samples were prepared using glycerol as the plasticizer. Different amounts of CAR (0, 10, and 30 wt%) were incorporated to AS matrix, namely, AS, AS-10CAR and AS-30CAR and three different amounts of MA (10, 15, and 20 wt%) were added to the blend of AS and CAR matrix, namely, AS-30CAR-10MA, AS-30CAR-15MA and AS-30CAR-20MA (Table 1). The film forming solutions were kept at a concentration of 7% (w/v) using 30 wt% of glycerol. The film solution was heated and stirred until the temperature reached 85°C for 15 min. Finally, the film solution was poured into PP trays and then dried at 60°C for 10 h.

Table 1 Compositions of different AS modified films.

Samples	AS (wt%)	CAR (wt%)	MA (wt%)
AS	100	-	-
AS-10CAR	90	10	-
AS-30CAR	70	30	-
AS-30CAR-10MA	70	30	10
AS-30CAR-15MA	70	30	15
AS-30CAR-20MA	70	30	20

2.4 FTIR

FTIR spectroscopic study was conducted to record IR spectra using a device called IRTracer-100 (Shimadzu, Japan). The scanning range spanned wavelengths from 4000 cm^{-1} to 700 cm^{-1} with a resolution of 4 cm^{-1} and 20 consecutive scans were taken to obtain the spectra.

2.5 XRD

A diffractogram was obtained by XRD-6100 (Shimadzu, Japan) using CuKα radiation operated at a wavelength of 1.54 Å, 40 kV and 30 mA, over an angular range of 2θ = 5° to 50°. The degree of crystallinity was then calculated using Equation (1) :

$$\text{Crystallinity (\%)} = \frac{Ac}{Ac+Aa} \times 100 \quad (1)$$

The crystalline region (2θ = 12° to 28°), denoted as Ac, and the amorphous region (2θ = 5° to 50°), denoted as Aa, were determined on the X-ray diffractogram.

2.6 Morphology

Cross-sectional morphology of a specimen was determined using a scanning electron microscope (SEM) (JSM-IT500HR, JEOL, LA) which operated at an accelerating voltage of 10 kV with 2000X magnification. The specimen was fractured under liquid nitrogen, fixed on a stub and coated by a thin gold film.

2.7 Mechanical properties

Mechanical properties of a sample was performed using a Universal testing machine (Cometech QC-536M1, Taiwan), equipped with 2 kN load cell and operated at 50 $mm \cdot min^{-1}$ crosshead speed, in accordance with ASTM D-882 standard. Prior to the test, the sample (100 × 15 mm^2) was kept at 60 ± 2% RH using a saturated ammonium nitrate solution. The mechanical tests were carried out at 23 ± 1°C and 60 ± 2% RH. The thickness of the film was in the range of 0.15 mm to 0.20 mm. At least twelve samples were used and the averaged values were, then, calculated.

2.8 Moisture uptake, WVTR and degree of swelling

The moisture uptake experiment involved drying a film at 105°C for 2 h and then storing it in a closed receptacle at 99 ± 1% RH. The moisture content absorbed by the sample was then measured over 7 days following ASTM D-570 method. Moisture uptake percentage was calculated using Equation (2) :

$$\text{Moisture uptake (\%)} = \frac{W_2-W_1}{W_1} \times 100 \quad (2)$$

where W_1 and W_2 were the dried and the wet weights of the sample, respectively.

The gravimetric modified cup method (ASTM E96) was used to determine WVTR. The process involved placing a sealed cup with the sample being tested (with an area of 19.63 cm^2) in a chamber with a constant 75% RH created by a saturated solution of sodium chloride. The cup was weighed and then re-weighed every 24 h for a period of 7 days. WVTR value was then calculated using Equation (3) :

$$\text{WVTR} = \frac{\Delta m}{(\Delta t \, .A)} \times 100 \quad (3)$$

where $\Delta m/\Delta t$ represented the weight gain of samples per day ($g \cdot day^{-1}$), and A denoted the permeative surface area of samples (cm^2).

For the determination of degree of swelling, a film (1 in × 1 in) was dried at 105°C for 2 h and then soaked in distilled water for 24 h at room temperature. The wet weight of the wet sample (W_2) was measured after blotting water from its surface. Swelling percentage was calculated as follows:

$$\text{Swelling (\%)} = \frac{W_2-W_1}{W_1} \times 100 \quad (4)$$

where W_1 and W_2 were the dried and the wet weights of the sample, respectively.

2.9 Antibacterial activity

The agar diffusion method was selected to examine antibacterial property of a film. Sample discs (with a diameter of 10 mm) were placed on agar plates containing gram-positive (*S.aureus*) and gram-negative (*E.coli*) strains, followed by incubation at 37°C for 24 h. The antibacterial property of the sample was examined by measuring the diameter of the inhibited zone.

2.10 In vitro cytotoxicity

MTT assay was used to conduct a cytotoxicity test on human keratinocyte (HaCat) cells. The sample (0.0115 ± 0.0007 g) was soaked in phosphate-buffered saline, filtered, and incubated (37°C, 24 h) with DMEM (Dulbecco's Modified Eagle Medium) and 10% FBS (Fetal Bovine Serum). HaCat cells (100 µL, 1 × 105 $cells \cdot mL^{-1}$) were seeded into each well of a 96-well plate and incubated (37°C, 24 h). The incubated filtrate mixture (100 mL) and MTT solution (5 $mg \cdot mL^{-1}$, 10 µL) were added and incubated at 37°C for 4 h. Subsequently, the solution of formazan dissolution was added to the well, and the resultant solution was measured for absorbance at 570 nm using a Biochrom microtiter plate reader. Cell morphology was determined using optical microscope images. The percentage of cytotoxicity and cell viability were calculated using Equations (5-6).

$$\text{Cytotoxicity (\%)} = ((A–B)/A) \times 100 \quad (5)$$

$$\text{Cell viability (\%)} = 100 – \text{Cytotoxicity} \quad (6)$$

where A represented the absorbance of the control well and B represented the absorbance of the test well.

2.11 Statistical Analysis

The analysis of variance (ANOVA) procedure was used to conduct statistical analysis with IBM SPSS statistics 25 software. Tukey's test was employed to assess differences among the means ($p < 0.05$).

3. Results and Discussion

Different biodegradable wound dressing films were prepared from modified cassava starch with VA resulted in the replacement of hydroxyl groups (-OH) in molecules of starch with acetyl groups (-$COCH_3$) from VA via acetylation reaction, yielding AS [7]. AS film modified by CAR could create hydrogen bonds between AS and CAR molecules. Furthermore, the stable structure of CAR (Figure 1(a)) caused by electrostatic interaction between potassium ion and sulfate groups on CAR chains promoted network structure formation [18]. Moreover, the addition of MA to the film (Figure 1(b)) may also result in forming hydrogen bonds between hydroxyl or carbonyl groups of MA molecules and hydroxyl groups of the matrix molecules.

3.1 FTIR

FTIR technique can be used to analyze functional groups of various AS films. FTIR spectrum of several AS films with different CAR and MA contents indicated polysaccharide characteristics, as shown in Figure 2 and all AS films represented resembling FTIR spectra. The FTIR main peak positions of AS films were located at 3600 cm^{-1} to 3200 cm^{-1}, 3000 cm^{-1} to 2800 cm^{-1}, 1485 cm^{-1} to 1425 cm^{-1}, 1300 cm^{-1} to 1000 cm^{-1} and 900 cm^{-1} to 700 cm^{-1} exhibited O–H stretching, C–H asymmetric stretching of $–CH_2–$ and $–CH_3–$, O–H bending, C–O–C stretching and C–O–C ring vibration of starch, respectively [26]. The peak position at 1724 cm^{-1} was caused by C=O stretching of acetyl groups from the acetylation [6, 25].

When CAR was incorporated into AS matrix (AS-CAR), the characteristic bands of CAR were strengthened at the peak positions of 1242 cm^{-1}, 923 cm^{-1} and 846 cm^{-1} contributed to the asymmetric stretching of O=S=O of ester sulfate groups, C–O–C stretching of 3,6-anhydrogalactose and C–O–S stretching of galactose-4-sulfate, respectively [27]. It was observed that the peak position at 3500 cm^{-1} to 3300 cm^{-1}, which was due to O–H stretching band shifted to lower wavenumbers, when increasing the amount of CAR. It was due to new hydrogen bonding interaction between hydroxyl groups of CAR and AS molecules. The result was similar to the research reported for hydrogen bond formation observed in starch-carboxymethyl cellulose (CMC) blend [28].

FTIR spectra of various AS films added with 30CAR and different MA contents (10, 15, and 20% w/w) were shown in Figure 2(b). It was observed that the wavenumber of O-H stretching band (3500 cm^{-1} to 3300 cm^{-1}) shifted to lower wavenumbers and the intensity of the wavenumber decreased (Figure 2(b) and Table 2) since hydroxyl or carbonyl groups of MA could form hydrogen bonding with hydroxyl group of the matrix molecule. Simultaneously, hydrolysis of the polymer matrix could also take place. Similar observation was found for corn starch/pullulan/gallic acid (CS/PUL/GA) films. It showed O–H stretching peak at 3350 cm^{-1} in CS/PUL/GA spectrum and shift a lower wavenumber due to the hydrogen bond between hydroxyl group of GA and CS/PUL [29]. Furthermore, the wavenumber at 1650 cm^{-1} to 1640 cm^{-1}, corresponded to C=C stretching of the aromatic MA was observed and this peak position confirmed the presence of MA in the film. In addition, the intensity of wavenumber at 1724 cm^{-1}, which was due to C=O stretching of both from AS and MA molecules [30]. Furthermore, the intensity of 1724 cm^{-1} tended to increase with the increasing content of MA.

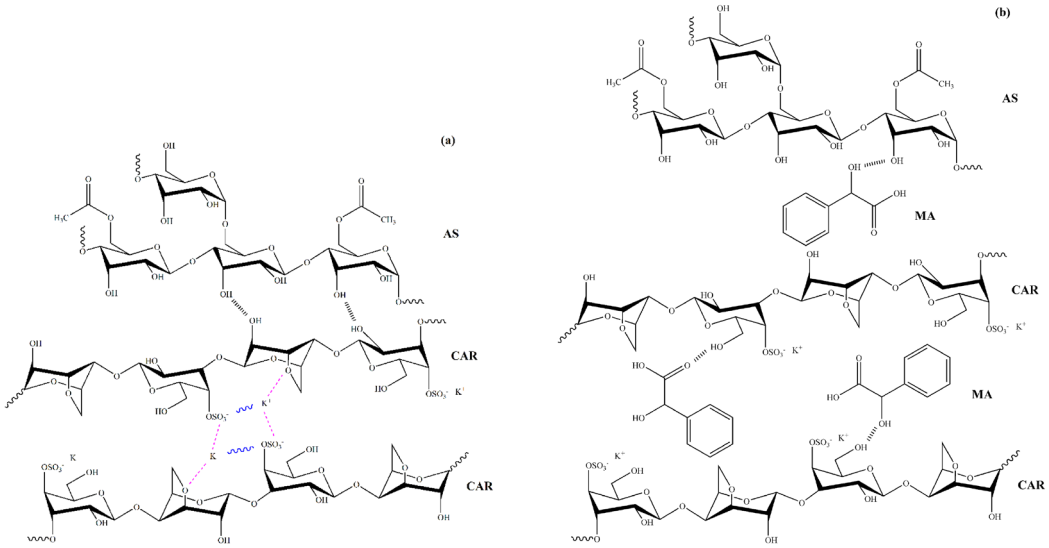

Figure 1 Possible interactions of modified AS films (a) AS-CAR film, and (b) AS-30CAR-MA film.

Table 2 Peak heights and ratios of peak heights of AS-30CAR-MA films.

Sample	Peak height		Ratio of peak height
	3500 cm^{-1} to 3300 cm^{-1}	846 cm^{-1}	3500 cm^{-1} to 3300 cm^{-1}/846 cm^{-1}
AS-30CAR	30.45	10.46	2.91
AS-30CAR-10MA	28.80	10.87	2.65
AS-30CAR-15MA	25.53	11.03	2.31
AS-30CAR-20MA	21.71	10.46	2.08

Remark: ratio of peak height = peak height of interested peak/peak height of referenced peak of 846 cm^{-1}.

3.2 XRD

Percentage of crystallinity for different AS films can be determined using XRD analysis, as shown in Table 3 and Figure 3. It was found that AS film exhibited the diffracted peak at 2θ of 20.2° corresponded to V- and E-type crystal structure [31]. The same diffracted peak appearance was also observed when CAR was incorporated into AS film (AS-CAR). However, the peak intensity and degree of crystallinity of AS-CAR films decreased significantly compared to AS film and this was because CAR was amorphous in nature [32]. Moreover, hydrogen bonding between hydroxyl groups of CAR and AS starch molecules could hinder the molecular arrangement of the starch, caused the drop of crystallinity of the film. Similar observation was reported for starch and CAR blend, and it was found that the crystallinity of the starch film reduced when CAR was increased [33].

When MA was incorporated into (AS-30CAR-MA) films, the new diffracted peaks were observed at 2θ values of 9.5° and 28.6° and these diffracted peaks confirmed the presence of MA in the film [34]. With the increasing amount of MA, it was observed that the peak intensity at 2θ of 9.5° and 28.6° was slightly increased while the intensity of the peak at 2θ of 20.2° was decreased. As a result, the increase of MA content resulted in partly interruption of the crystallization in the polymer matrix.

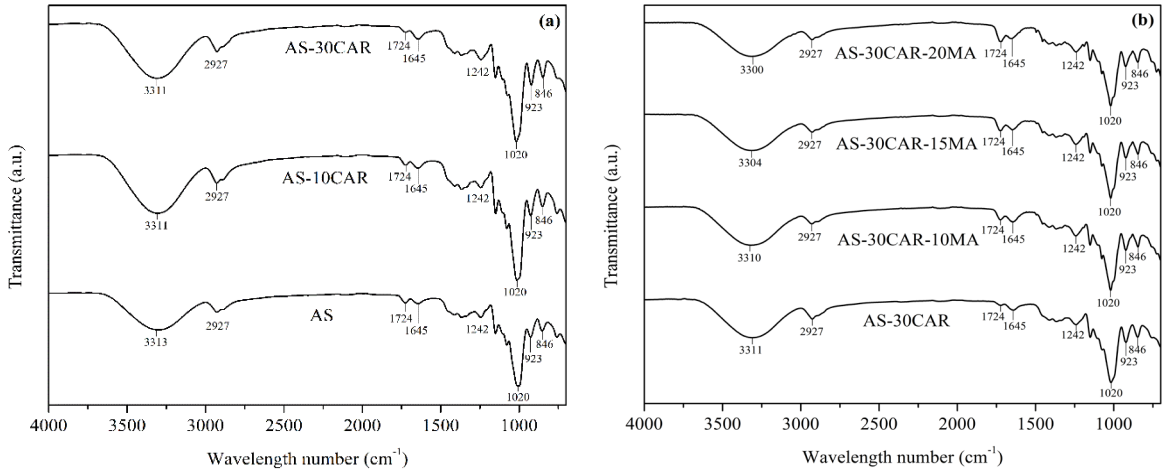

Figure 2. FTIR spectra of (a) AS and AS-CAR films, and (b) AS-30CAR films with different contents of MA.

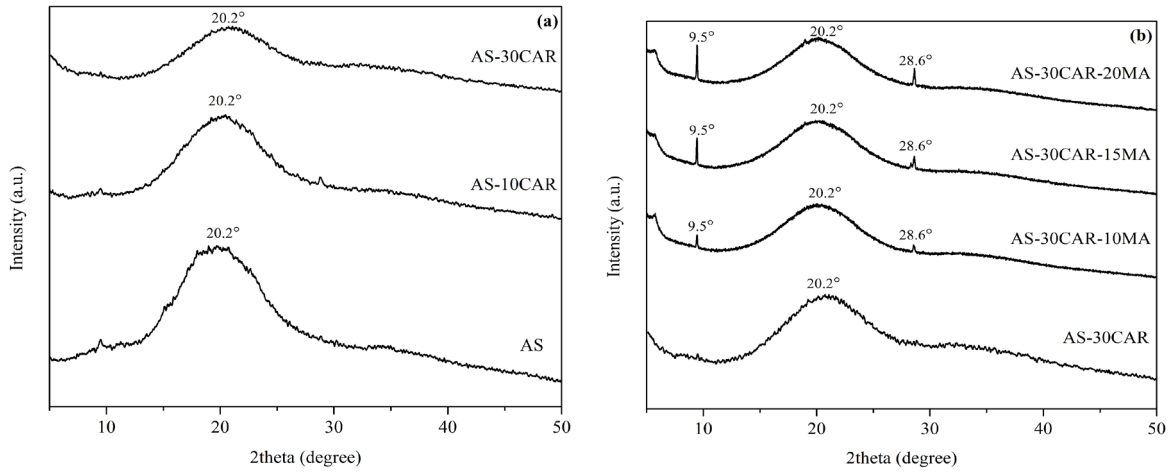

Figure 3 X-ray diffractograms of (a) AS and AS-CAR films, and (b) AS-30CAR films with different contents of MA.

Table 3 Percentage of crystallinity and mechanical properties of AS films with different contents of CAR and MA.

Samples	Crystallinity (%)	Maximum stress (MPa)	Elastic modulus (MPa)	Maximum strain (%)
AS	33.82	1.13 ± 0.13^{a}	5.66 ± 1.39^{a}	172.16 ± 2.57^{a}
AS-10CAR	29.87	2.21 ± 0.07^{b}	25.33 ± 0.90^{b}	60.51 ± 2.3^{b}
AS-30CAR	21.88	5.24 ± 0.17^{c}	105.69 ± 2.32^{c}	44.47 ± 2.37^{b}
AS-30CAR-10MA	21.63	1.55 ± 0.08^{d}	26.52 ± 3.28^{b}	96.79 ± 7.46^{c}
AS-30CAR-15MA	20.44	0.76 ± 0.05^{e}	12.14 ± 0.37^{d}	106.20 ± 9.62^{c}
AS-30CAR-20MA	18.80	0.71 ± 0.04^{e}	10.81 ± 1.05^{d}	170.44 ± 17.14^{a}

Based on Tukey's test, different superscripts in the same column are significantly different ($p < 0.05$).

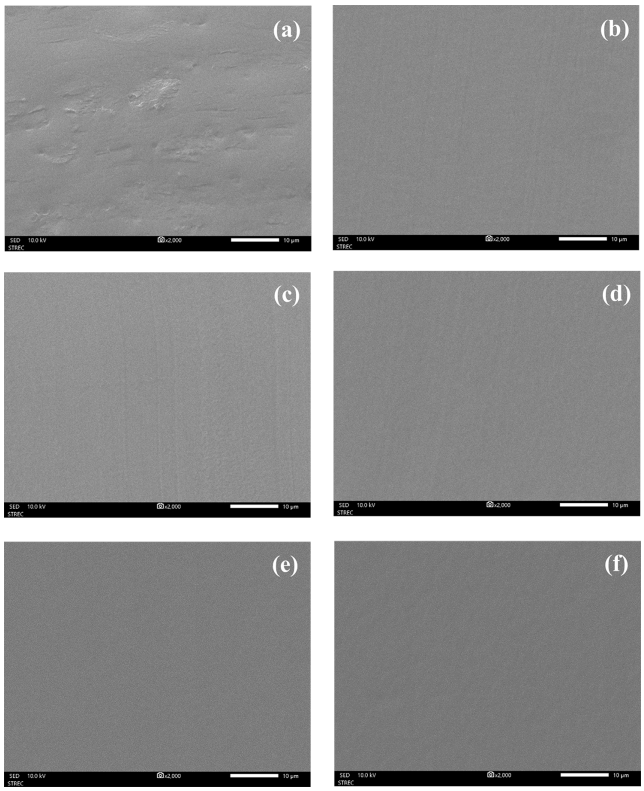

Figure 4 Cross-section characteristics of various AS films (a) AS, (b) AS-10CAR, (c) AS-30CAR, (d) AS-30CAR-10MA, (e) AS-30CAR-15MA, and (f) AS-30CAR-20MA.

3.3 Morphology

Figure 4 shows morphology of several AS films determined by SEM technique. The cross-section morphology of AS samples (Figure 4(a)) was homogeneous, with some rough area. For AS-CAR films (Figure 4(b-c)) smoother and more homogeneous cross-sectional surface were observed, as compared to AS film (Figure 4(a)). This was because the similar chemical structures of both AS and CAR, caused the good phase compatibility. Additionally, due to the amorphous characteristics of CAR, the increasing amount of CAR brought about the smooth of the films. When MA was added to AS-30CAR-MA films (Figure 4(d-f)), the cross-sectional surface of the sample exhibited similar characteristics as AS-CAR film, i.e., smooth and homogeneous surface. This result also indicated the good phase compatibility among AS, CAR, and MA molecules.

3.4 Mechanical properties

Table 3 represents mechanical properties, i.e., maximum stress, elastic modulus, and maximum strain of various AS films. It was detected that both maximum stress and elastic modulus clearly increased but the maximum strain decreased when CAR was incorporated into AS matrix (AS-CAR). Even though the addition of CAR into AS caused the reduction of starch crystallinity, as shown in Figure 3(a) and Table 3, the formation of hydrogen bonding interactions between hydroxyl groups of CAR and AS brought about strong intermolecular forces. Moreover, the electrostatic interactions within CAR molecules (Figure 1), caused by the counterion between potassium ions and sulfate groups, decreased the chain mobility of the polymer matrix, leading to the increased film stiffness.

Furthermore, maximum stress and elastic modulus also increased when CAR contents increased. This result was caused by both hydrogen bonds between AS and CAR molecules (as confirmed by FTIR) and electrostatic interactions within CAR molecules, resulting in the increase of stress transfer and stiffness of the films. Although the crystallinity of AS-CAR films decreased as CAR contents rose, the addition of CAR could improve phase compatibility between AS and CAR, resulting in smooth fractured surface of AS-CAR films, as shown in SEM micrograph (Figure 4). Similar reports were mentioned that not only the incorporation of CAR into starch-carboxymethyl cellulose (CMC) but also the addition of ι-carrageenan into arrowroot starch led to the increment of tensile strength and elastic modulus and the reduction of strain at break [28,32]. Therefore, AS-30CAR film with the highest maximum stress and elastic modulus value was chosen to be modified by MA.

Additionally, AS-30CAR-MA films, showed the reduction of maximum stress and elastic modulus, but the increment of elongation of maximum load (Table 3), compared with AS-30CAR film. Similar trends were detected for MA and salicylic acid added in soy protein films [22,35]. It was expected that hydroxyl or carbonyl groups of MA could form hydrogen bonding with hydroxyl group of the matrix molecule (Figure 2(b) and Table 2). Simultaneously, MA could also cause the hydrolysis reaction within the polymer matrix. Moreover, MA molecules disrupted the crystallization of AS chains and diminished hydrogen bonds and electrostatic interactions between AS-CAR and CAR-CAR (Figure 3 and Table 3). This reason caused the drop of maximum stress and elastic modulus. Furthermore, the increment of MA amount would result in the decrease of hydrogen bonding between intermolecular chains between AS and CAR, causing the drop of stress transfer among the polymer chains.

3.5 Moisture uptake, WVTR and degree of swelling

High water absorbency is one of the desirable properties of a wound dressing film. Table 4 presents the values of moisture uptake, WVTR, and degree of swelling for AS and different modified AS films. It can be seen that the addition of CAR into AS film significantly increased moisture uptake, WVTR, and degree of swelling. This influence could be due to the hydrophilic characteristics of CAR composed of sulfate groups and the decrease of crystallinity in AS-CAR film (Table 3) when compared to AS film, which enhanced the water-absorbed capacity of AS-CAR film. Moreover, the increased CAR content reduced intermolecular interactions within AS chains, resulting in an expanded polymer network structure. Similar observations were reported for both arrowroot starch blended with ι-carrageenan and cassava starch/PVA blended with CAR led to the increment of degree of swelling [18,32]. As a result, AS-30CAR film with the highest moisture uptake, WVTR, and degree of swelling values was selected to be incorporated with MA.

For AS-30CAR-MA films, according to Table 4, the moisture uptake, WVTR, and degree of swelling of the films decreased significantly. This was likely due to hydrophobic aryl groups of MA, which were water-repellent and caused the reduction of water absorption of AS modified film. Similar observation was reported for soy

protein and MA blend, and it was found that the water uptake of films reduced, resulting from aromatic groups [22]. Since hydrogen bonding between the polymer matrix (AS and CAR) and MA including electrostatic bond in its CAR structure were inhibited by the addition of MA, therefore, more void could be created. Consequently, AS-30CAR-10MA films clearly exhibited the decreased affinity for water. With the increasing amount of MA in AS-30CAR-MA films, it was found that the moisture uptake, WVTR, and degree of swelling of the film tended to increase slightly. This was expected because of the excessive MA disrupted the structure of matrix network. As the amount of MA increased, it hindered the occurrence of intermolecular interactions between the matrix chains, resulting in the increased distance between the chains. Consequently, water could easily penetrate the chains led to the increase of the moisture uptake, WVTR, and degree of swelling of different AS-30CAR-MA films. Similar values for moisture uptake and degree of swelling were reported for silk/ sodium alginate film, bacterial cellulose/chitosan/mangosteen extract film and sodium alginate/silver chloride film [36-38].

3.6 Antibacterial activity

The result of the antibacterial property of various AS samples incorporated with 30CAR and various MA contents MA (10, 15, and 20% wt) is shown in Figure 5 and Table 5. As expected, AS and AS-30CAR films, without MA, presented no antibacterial activity. However, AS-30CAR-15MA and AS-30CAR-20MA films showed effective antibacterial activity against *S.aureus* (Gram-positive) bacteria after being incorporated with MA. It should be noted that, only AS-30CAR-20MA film showed effective antibacterial activity against both grams of bacteria (*S.aureus* and *E.coli*). The result indicated that the increasing loadings of MA caused the improved antibacterial activity.

It was reported that MA presented the successful antibacterial activity against both *S.aureus* and *E.coli* bacteria. MA could interact with the protein and enzymes of bacteria by damaging the plasma membrane and resulting in intracellular substance leakage. At the same time, MA caused the change of the trans-membrane pH gradient between the organelle membranes and plasma membrane and disturb membrane function, causing deformation in structure and functionality [39,40].

Furthermore, MA presented effective antibacterial property against Gram-positive bacteria than Gram-negative bacteria. This was because Gram-negative bacteria were less susceptible to antibacterial agents than Gram-positive bacteria. Gram-negative bacteria are composed of complex double-layered cell wall with polysaccharides that inhibit the penetration of antibacterial agents. In contrast, Gram-positive bacteria have a single thick cell wall layer that is peptidoglycan, which is less complicated. These results made the antibacterial agents efficiently diffused through the cells, causing cell destruction and cell death [41].

3.7 In vitro cytotoxicity

MTT assay was performed to compare the cytotoxicity and cell viability of various AS films using HaCat cells. As shown in Figure 6 and Table 5. Comparison between AS and AS-30CAR films, the former exhibited lower cytotoxicity value and higher cell viability value, resulting from the toxicity of VA that was used to synthesize AS. Similarly, the MA addition to AS-30CAR specimens brought about the slight increase of cytotoxicity and the slight decrease of cell viability. However, the cell viability of all AS films still remained above 80%, indicating the non-toxic response to human cells, as indicated by ISO 10993-5 standard [42].

Table 4 Moisture uptake, WVTR and Degree of swelling of AS films with different contents of CAR and MA.

Samples	Moisture uptake (%)		WVTR ($gm^{-2}day^{-1}$)	Degree of swelling (%)	
	Day 4	Day 7		1 h	6 h
AS	31.91 ± 5.26^{a}	44.19 ± 6.99^{a}	326.31 ± 3.31^{a}	276.94 ± 2.13^{a}	495.36 ± 8.46^{a}
AS-10CAR	34.95 ± 4.84^{ab}	47.74 ± 2.71^{ab}	353.89 ± 5.50^{a}	265.11 ± 3.06^{a}	558.96 ± 5.08^{ab}
AS-30CAR	51.69 ± 1.93^{c}	64.65 ± 0.98^{c}	412.49 ± 8.52^{ab}	269.41 ± 6.43^{a}	641.28 ± 6.76^{b}
AS-30CAR-10MA	44.31 ± 2.00^{bc}	56.82 ± 3.07^{bc}	254.89 ± 7.12^{b}	173.68 ± 9.24^{b}	287.41 ± 3.00^{c}
AS-30CAR-15MA	44.89 ± 1.55^{c}	58.48 ± 2.25^{c}	274.89 ± 7.14^{b}	179.77 ± 5.65^{b}	307.81 ± 1.06^{c}
AS-30CAR-20MA	48.52 ± 3.26^{c}	61.68 ± 3.50^{c}	314.00 ± 3.50^{a}	181.33 ± 7.45^{b}	313.45 ± 4.29^{c}
Control (without film)			583.07 ± 3.08		

Based on Tukey's test, different superscripts in the same column are significantly different ($p < 0.05$).

Table 5 Inhibited zone, cytotoxicity and cell viability of different AS films.

Samples	**Inhibited zone (mm)**		**Cytotoxicity**	**Cell viability**
	S.aureus	***E.coli***	**(%)**	**(%)**
AS	Inactive	Inactive	12.65	87.35
AS-30CAR	Inactive	Inactive	3.33	96.67
AS-30CAR-10MA	Inactive	Inactive	14.51	85.49
AS-30CAR-15MA	15.74	Inactive	17.63	82.37
AS-30CAR-20MA	24.06	18.22	19.86	80.14
Control			5.52	94.45

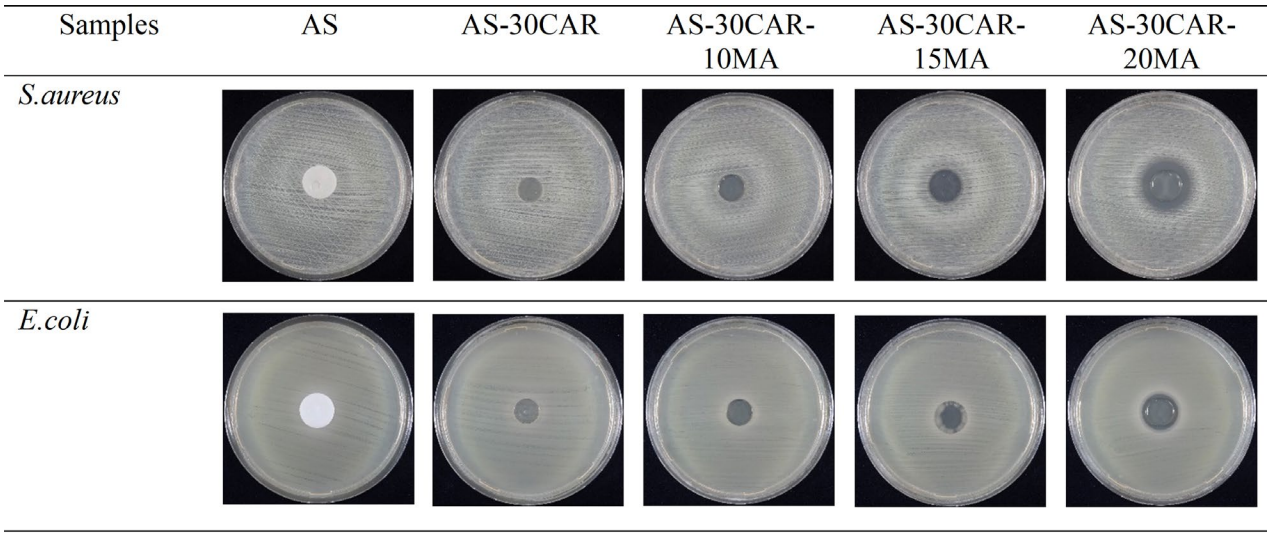

Figure 5 Inhibited zones different AS films against *S.aureus* and *E.coli*.

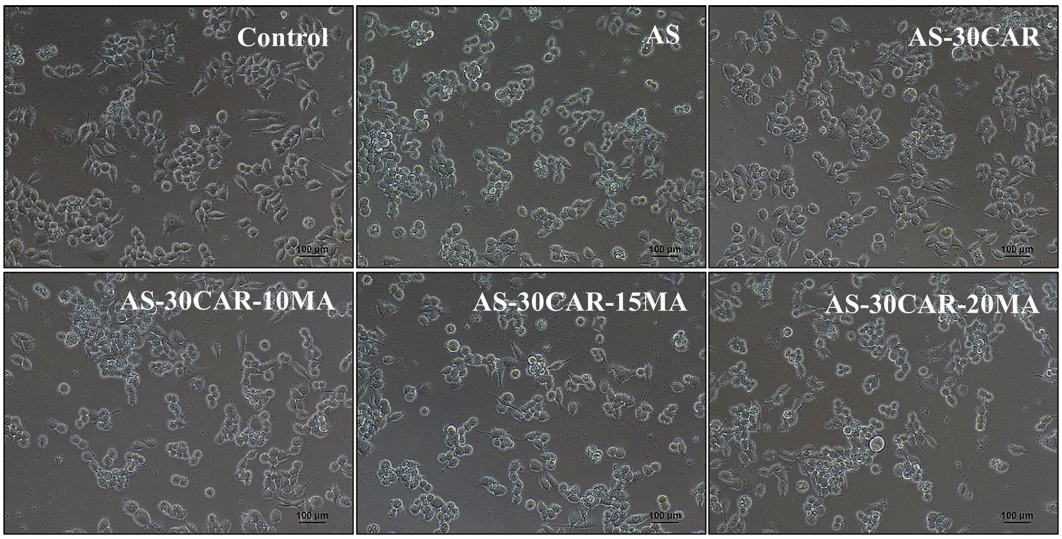

Figure 6 Optical micrographs of HaCat cells incubated after 24 h of different AS films.

4. Conclusion

The natural wound dressing films was successfully prepared by AS modified by CAR, and MA. The incorporation of CAR in AS caused FTIR peak position at 3500 cm^{-1} to 3300 cm^{-1}, assigned for O–H stretching, shifted to lower wavenumbers because of new hydrogen bond formation between AS and CAR. SEM images showed smoother and more homogeneous cross-sectional surface as compared to AS film. Eventhough, the crystallinity, determined for the starch crystallinity, of the blended film was decreased, but the significant rise of maximum stress, elastic modulus, moisture uptake, WVTR, and degree of swelling were observed because of hydrogen bonding and electrostatic interaction between AS and CAR. However, the increased content of MA caused the reversed effect, i.e. moisture uptake, WVTR, degree of swelling were increased, but maximum stress and elastic modulus were decreased. When MA was added into AS-30CAR film, it caused the improvement of antibacterial properties against *S. aureus* in AS-30CAR-15MA and AS-30CAR-20MA films. Moreover, AS-30CAR-20MA film presented the most effective antibacterial property against both *S. aureus* and *E. coli*. In addtion, all AS modified films showed no cytotoxicity to HaCat cells. In this study, AS-30CAR-20MA film was suitable for wound dressing application since it showed the improvement of elastic modulus, moisture uptake and antibacterial activity compared to AS film.

Acknowledgements

The authors express their sincere appreciation to King Mongkut's Institute of Technology Ladkrabang (Grant No. 2566-02-05-009) for financial support and to School of Science for facility support.

References

[1] H. R. Rashdan and M. E. El-Naggar, "Traditional and modern wound dressings—characteristics of ideal wound dressings," in *Antimicrobial Dressings*, K. Raju and G. Sorna, Eds. Massachusetts: Academic Press, 2023, pp. 21-41.

[2] I. Savencu, S. Iurian, A. Porfire, C. Bogdan, and I. Tomuță, "Review of advances in polymeric wound dressing films," *Reactive and Functional Polymers,* vol. 168, p. 105059, 2021.

[3] C. Wang, Y. Lu, Z. Li, X. An, Z. Gao, and S. Tian, "Preparation and performance characterization of a composite film based on corn starch, κ-carrageenan, and ethanol extract of onion skin," *Polymers,* vol. 14, no. 15, p. 2986, 2022.

[4] S. Chuayjuljit, S. Hosililak, and A. Athisart, "Thermoplastic cassava starch/sorbitol-modified montmorillonite nanocomposites blended with low density polyethylene: properties and biodegradability study," *Journal of Metals, Materials and Minerals,* vol. 19, 2009.

[5] R. Colussi, S. L. M. El Halal, V. Z. Pinto, J. Bartz, L. C. Gutkoski, E. da Rosa Zavareze and A. R. G. Dias, "Acetylation of rice starch in an aqueous medium for use in food," *LWT - Food Science and Technology,* vol. 62, no. 2, pp. 1076-1082, 2015.

[6] F. Han, M. Liu, H. Gong, S. Lü, B. Ni, and B. Zhang, "Synthesis, characterization and functional properties of low substituted acetylated corn starch," *International Journal of Biological Macromolecules,* vol. 50, no. 4, pp. 1026-1034, 2012.

[7] A. Ayucitra, "Preparation and characterisation of acetylated corn starches," *International Journal of Chemical Engineering and Applications,* vol. 3, no. 3, p. 156, 2012.

[8] I. A. Wani, D. S. Sogi, and B. S. Gill, "Physico-chemical properties of acetylated starches from Indian black gram (*Phaseolus mungo L.*) cultivars," *Journal of food science and technology,* vol. 52, pp. 4078-4089, 2015.

[9] S. Mehboob, T. M. Ali, M. Sheikh, and A. Hasnain, "Effects of cross linking and/or acetylation on sorghum starch and film characteristics," *International journal of biological macromolecules,* vol. 155, pp. 786-794, 2020.

[10] N. E. Kochkina, O. A. Butikova, and N. D. Lukin, "Ecofriendly films based on low-substituted starch acetate enhanced by polyvinyl alcohol additions," *Iranian Polymer Journal,* vol. 31, no. 11, pp. 1361-1371, 2022.

[11] E. J. Jiménez-Regalado, C. Caicedo, A. Fonseca-García, C. C. Rivera-Vallejo, and R. Y. Aguirre-Loredo, "Preparation and physicochemical properties of modified corn starch–chitosan biodegradable films," *Polymers,* vol. 13, no. 24, p. 4431, 2021.

[12] R. O. Sonawane, and S. D. Patil, "Gelatin–κ-carrageenan polyelectrolyte complex hydrogel compositions for the design and development of extended-release pellets," *International Journal of Polymeric Materials and Polymeric Biomaterials,* vol. 66, no. 16, pp. 812-823, 2017.

[13] E. Abdou, and M. Sorour, "Preparation and characterization of starch/carrageenan edible films," *International food research journal,* vol. 21, no. 1, pp. 189-193, 2014.

[14] Y. Zhou, F.-Q. Chen, S. Chen, Q. Xiao, H.-F. Weng, Q.-M. Yang, and A.-F. Xiao, "Preparation and characterization of κ-carrageenan modified with maleic anhydride and its application in films," *Marine Drugs,* vol. 19, no. 9, p. 486, 2021.

[15] S. Mohandoss, S. Ganesan, K. Velsankar, S. Sudhahar, F. H. Alkallas, A. B. G. Trabelsi, F. V. Kusmartsev, H. M. Lo and Y. R. Lee, "Fabrication and characterization of Ag nanoparticle-embedded kappa-Carrageenan-Sodium alginate nanocomposite hydrogels with potential antibacterial and cytotoxic activities," *Journal of Biomaterials Science, Polymer Edition,* vol. 34, no. 6, pp. 715-733, 2023.

[16] A. C. Flores, E. R. Punzalan, and N. G. Ambangan, "Effects of kappa-carrageenan on the physico-chemical properties of thermoplastic starch," *Kimika,* vol. 26, no. 1, pp. 10-16, 2015.

[17] J. W. Rhim, "Physical-mechanical properties of agar/κ-carrageenan blend film and derived clay nanocomposite film," *Journal of Food Science,* vol. 77, no. 12, pp. 66-73, 2012.

[18] C. de Lima Barizão, M. I. Crepaldi, S. Oscar de Oliveira, A. C. de Oliveira, A. F. Martins, P. S. Garcia and E. G. Bonafé, "Biodegradable films based on commercial κ-carrageenan and cassava starch to achieve low production costs," *International Journal of Biological Macromolecules,* vol. 165, pp. 582-590, 2020.

[19] D. Tungmunnithum, A. Thongboonyou, A. Pholboon, and A. Yangsabai, "Flavonoids and other phenolic compounds from medicinal plants for pharmaceutical and medical aspects: An overview," *Medicines,* vol. 5, no. 3, p. 93, 2018.

[20] O. Zavyalova, S. Gajewska, D. Dąbrowska-Wisłocka, and A. Sionkowska, "Characteristics of physicochemical and rheological properties of chitosan hydrogels based on selected hydroxy acids," *Engineering of Biomaterials,* vol. 24, no. 161, 2021.

[21] R. Kumar and P. Rani, "Mandelic acid incorporated antimicrobial soy protein film fabricated by solution casting," in *Advances in Polymer Sciences and Technology, Materials Horizons: From Nature to Nanomaterials*, B. Gupta, A. Ghosh, A. Suzuki, S. Rattan, Eds. Singapore: Springer, 2018, pp. 13-19.

[22] R. Kumar, R. D. Anandjiwala, and A. Kumar, "Thermal and mechanical properties of mandelic acid-incorporated soy protein films," *Journal of Thermal Analysis and Calorimetry,* vol. 123, no. 2, pp. 1273-1279, 2015.

[23] M. Motamedifar, A. Bazargani, M. R. Namazi, E. Sarai, and H. Sedigh, "Antimicrobial activity of mandelic acid against methicillin-resistant Staphylococcus aureus: a novel finding with important practical implications," *World Applied Sciences Journal,* vol. 31, no. 5, pp. 925-929, 2014.

[24] C. S. Raina, S. Singh, A. S. Bawa, and D. C. Saxena, "Some characteristics of acetylated, cross-linked and dual modified Indian rice starches," *European Food Research and Technology,* vol. 223, no. 4, pp. 561-570, 2006.

[25] D. Kalita, N. Kaushik, and C. L. Mahanta, "Physicochemical, morphological, thermal and IR spectral changes in the properties of waxy rice starch modified with vinyl acetate," *Journal of Food Science and Technology,* vol. 51, pp. 2790-2796, 2014.

[26] A. H. D. Abdullah, S. Chalimah, I. Primadona, and M. H. G. Hanantyo, "Physical and chemical properties of corn, cassava, and potato starchs," *IOP Conference Series: Earth and Environmental Science,* vol. 160, p. 012003, 2018.

[27] R. Wang, S. Zhang, S. Liu, Y. Sun, and H. Xu, "A contribution to improve barrier properties and reduce swelling ratio of κ-carrageenan film from the incorporation of guar gum or locust bean gum," *Polymers,* vol. 15, no.7, p. 1751, 2023.

[28] A. H. Dawam Abdullah, B. Firdiana, R. Choerun Nissa, R. Satoto, M. Karina, D. Fransiska, Nurhayati, Agusman, H. E.

Irianto, P. Priambudi, S. Marliah and Ismadi, "Effect of k-carrageenan on mechanical, thermal and biodegradable properties of starch–carboxymethyl cellulose (CMC) bioplastic," *Cellulose Chemistry and Technology,* vol. 55, pp. 1109-1117, 2021.

[29] M. Zhang, B. Yang, Z. Yuan, Q. Sheng, C. Jin, J. Qi, M. Yu, Y. Liu, G. Xiong, "Preparation and performance testing of corn starch/pullulan/gallic acid multicomponent composite films for active food packaging," *Food Chemistry: X,* vol. 19, p. 100782, 2023.

[30] M. Leon-Bejarano, Y. Durmus, M. Ovando-Martínez, and S. Simsek, "Physical, barrier, mechanical, and biodegradability properties of modified starch films with nut by-products extracts," *Foods,* vol. 9, no. 2, p. 226, 2020.

[31] N. Noivoil and R. Yoksan, "Compatibility improvement of poly(lactic acid)/thermoplastic starch blown films using acetylated starch," *Journal of Applied Polymer Science,* vol. 138, no. 2, p. 49675, 2020.

[32] A. A. Abdillah and A. L. Charles, "Characterization of a natural biodegradable edible film obtained from arrowroot starch and iota-carrageenan and application in food packaging," *International Journal of Biological Macromolecules,* vol. 191, pp. 618-626, 2021.

[33] A. Hartiati, B. A. Harsojuwono, H. Suyanto, and I. W. Arnata, "Characteristics of starch-based bioplastic composites in the ratio variations of the polysaccharide mixture," *International Journal of Pharmaceutical Research,* vol. 13, no. 2, 2021.

[34] L. Fitriani, H. Fadina, H. Usman, and E. Zaini, "Formation and characterization of multicomponent crystal of trimethoprim and mandelic acid by solvent drop grinding method," *International Journal of Applied Pharmaceutics,* pp. 75-79, 2023.

[35] H. Bai, R. Kumar, C. Yang, X. Liu, and L. Zhang, "Effect of salicylic acid on the mechanical properties and water resistance of soy protein isolate films," *Polymers and Polymer Composites,* vol. 18, no. 4, pp. 197-203, 2010.

[36] S. Nachiappan, L. Amanuel, T. Agazie, and S. Bihonegn, "Development and characterization of silk films for burn wound healing," *Research Journal of Textile and Apparel,* vol. 24, pp. 131-146, 2020.

[37] P. Moonsungnoen, D. Ochaikul, and P. Monvisade, "Bacterial cellulose and bacterial cellulose/chitosan films containing mangosteen pericarp extract for wound dressings," *Chiang Mai Journal of Science,* vol. 48, no. 4, pp. 952-968, 2021.

[38] M. Puccetti, A. Donnadio, M. Ricci, L. Latterini, G. Quaglia, D. Pietrella, A. D. Michele and V. Ambrogi, "Alginate Ag/Agcl nanoparticles composite films for wound dressings with antibiofilm and antimicrobial activities," *Journal of Functional Biomaterials,* vol. 14, no. 2, p. 84, 2023.

[39] Y. Fang, J. Fu, C. Tao, P. Liu, and B. Cui, "Mechanical properties and antibacterial activities of novel starch-based composite films incorporated with salicylic acid," *International journal of biological macromolecules,* vol. 155, pp. 1350-1358, 2020.

[40] X. Hu, L. Yuan, L. Han, S. Li, and L. Song, "Characterization of antioxidant and antibacterial gelatin films incorporated with Ginkgo biloba extract," *RSC advances,* vol. 9, no. 47, pp. 27449-27454, 2019.

[41] T. J. Gutiérrez, P. G. Seligra, C. M. Jaramillo, L. Famá, and S. Goyanes, "Effect of filler properties on the antioxidant response of thermoplastic starch composites," *Handbook of composites from renewable materials, structure and chemistry,* V. K. Thakur, M. K. Thakur and M. R. Kessler, Eds. New Jersey: Wiley, 2017, pp. 337-370.

[42] K. M. Zepon, M. M. Martins, M. S. Marques, J. M. Heckler, F. D. P. Morisso, M. G. Moreira, A. L. Ziulkoski and L. A. Kanis, "Smart wound dressing based on κ–carrageenan/locust bean gum/cranberry extract for monitoring bacterial infections," *Carbohydrate polymers,* vol. 206, pp. 362-370, 2019.